Light-front approach to hadron structures with quantum computing

Wenyang Qian

In collaboration with Robert Basili, Soham Pal, Glenn Luecke, James Vary,

Iowa State University, Ames, IA, USA

The Quantumness of Hard Probes YOUNGST@RS - MITP

01/19/2022 at 10:30 AM (US Central)

Outline

1. Introduction to quantum computing
   - Background

2. Light-front Hamiltonian approach
   - Effective light-front Hamiltonian
   - Meson spectroscopy and observables

3. Application of quantum computing
   - Problem formulation
   - Qubit encoding and unitary ansatz
   - Results of spectroscopy
   - Results of observables

Introduction to Quantum Computing

❖ Classical computers:
- classical bit: 0, 1
- implementation: electric voltage Low, High
- classical gates: AND, OR, NOT, Bitwise logic gates
- deterministic nature

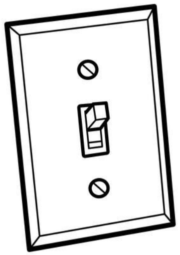

❖ Quantum computers:
- quantum bit (qubit): $|0\rangle = \begin{pmatrix} 1 \\ 0 \end{pmatrix}, |1\rangle = \begin{pmatrix} 0 \\ 1 \end{pmatrix}$
- implementation: two-level quantum systems

$$|\Psi\rangle = \alpha|0\rangle + \beta|1\rangle, \; |\alpha|^2 + |\beta|^2 = 1$$

- quantum gates: unitary operators
- <u>superposition</u>
- states only collapse when measured
- can theoretically solve problems classical computers cannot solve

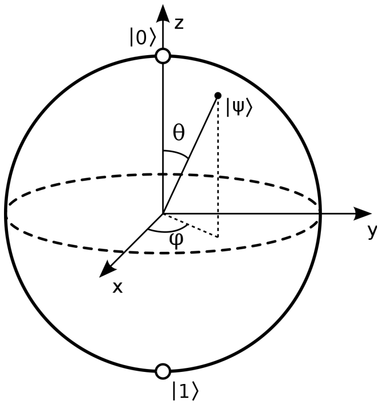

Developments in Quantum Computing

Quantum computing has come a long way in past 40 years

- Quantum implementation of Toffoli Gate (1980)
- Deutsch-Jozsa Algorithm: First example of quantum algorithm that is exponentially faster (1992)
- Shor's Algorithm: Factoring large numbers (1994)
- Quantum Error Correction (1995)
- Transmon Qubits (2007)
- Variational Quantum Eigensolver: broad applications in quantum chemistry (2014)
- Quantum Machine Learning: Quantum classifier, Quantum Support Vector Machines, Quantum Approximation Optimization, etc (2017)

Noisy Intermediate-Scale Quantum (NISQ): those devices whose qubits and quantum operations are substantially imperfect. [Preskill, 2018] [Bharti, 2101.08448]

Quantum advantage: a purpose-specific computation that involves a quantum device and that can not be performed classically with a reasonable resources. [Google AI, Arute 2019] [UTSC, Zhong 2020]

Major areas of **quantum computing applications** include:

- Quantum Fourier transform (quantum arithmetic, phase estimation)
- Quantum search algorithm (Grover's algorithm)
- **Quantum simulations** (**VQE**, QAOA)

…

Why are we interested?

- *"Nature isn't classical, dammit, and if you want to make a simulation of nature, you'd better make it quantum mechanical"* (Richard Feynman)

  Many problems are inherently quantum mechanical.

- Vast amount of encoded information in a many-qubit state: the total state space of n-qubit goes with 2^n

- High scalability in quantum applications (compact encoding)

- Many-body problems and quantum computing are similar by nature

- Rapid progress in quantum hardware

  (~100 qubits, improved scale, quality and speed) [IBM, 2110.14108]

Light-front Hamiltonian formalism

Basis Light-front Quantization (BLFQ) [Vary, 0905.1411]

- ❖ Light-front dynamics
  simple dispersion relation
- ❖ Hamiltonian approach
  eigenvalues => mass spectrum
  eigenfunctions => observables
- ❖ Basis function approach
  exploit symmetry

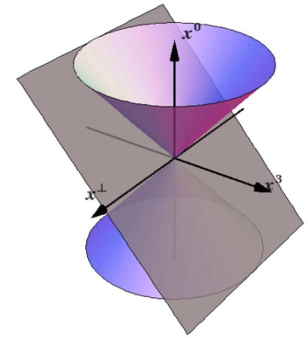

front form

In the application of the light mesons within the valence $|q\bar{q}\rangle$ Fock sector

[Qian, 2005.13806]

$$H_{\mathrm{eff},\gamma_5} = \overbrace{\underbrace{\frac{\mathbf{k}_\perp^2 + m_q^2}{x} + \frac{\mathbf{k}_\perp^2 + m_{\bar{q}}^2}{1-x}}_{\text{LF kinetic energy}} + \underbrace{\kappa^4 x(1-x)\mathbf{r}_\perp^2 - \frac{\kappa^4}{(m_q+m_{\bar{q}})^2}\frac{\partial}{\partial x}\left(x(1-x)\frac{\partial}{\partial x}\right)}_{\text{confinement}}}^{H_{\mathrm{eff}}} + \underbrace{V_g}_{\text{one-gluon exchange}} + H_{\gamma_5}$$

m_q $(m_{\bar{q}})$ is the mass of the quark/antiquark, κ is the confining strength

V_g is the one-gluon exchange, H_{γ_5} is the pseudoscalar contact interaction

[Li, 1704.06968]

Light meson spectrum and wave functions

Transverse and longitudinal basis functions are truncated with $N_{\max}$ (basis energy scale) and $L_{\max}$ (longitudinal resolution) for the light-front wave functions (LFWFs) :

$$\psi_{s\bar{s}}^{m_j}(\boldsymbol{k}_\perp, x) = \sum_{nml} \tilde{\psi}_{s\bar{s}}^{m_j}(n,m,l)\phi_{nm}\left(\frac{\boldsymbol{k}_\perp}{\sqrt{x(1-x)}}\right)\chi_l(x)$$

2D harmonic oscillator *Jacobi polynomial*

$$2n + |m| + 1 \leq N_{\max}$$
$$l \leq L_{\max}$$

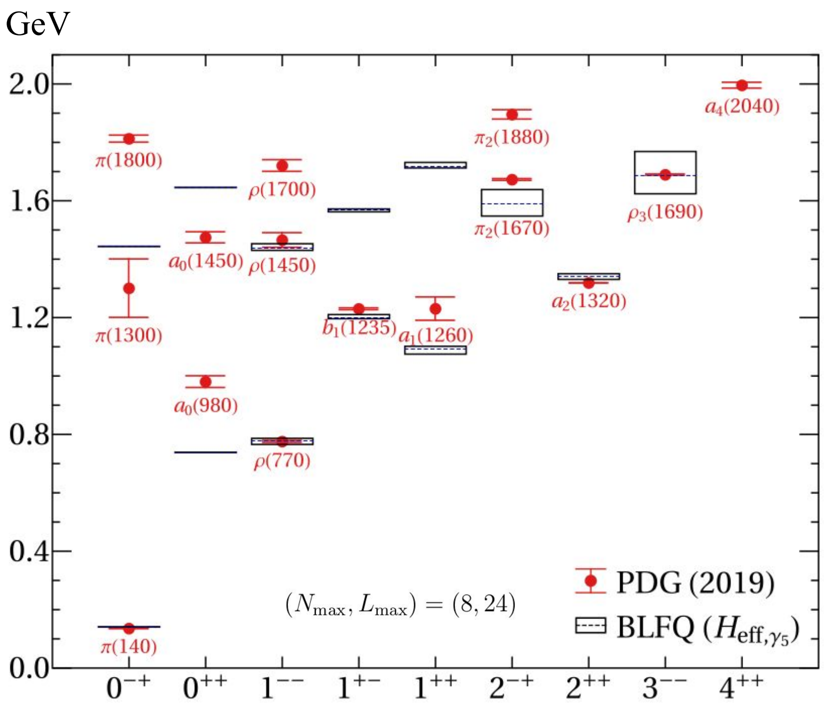

[Qian, 2005.13806]

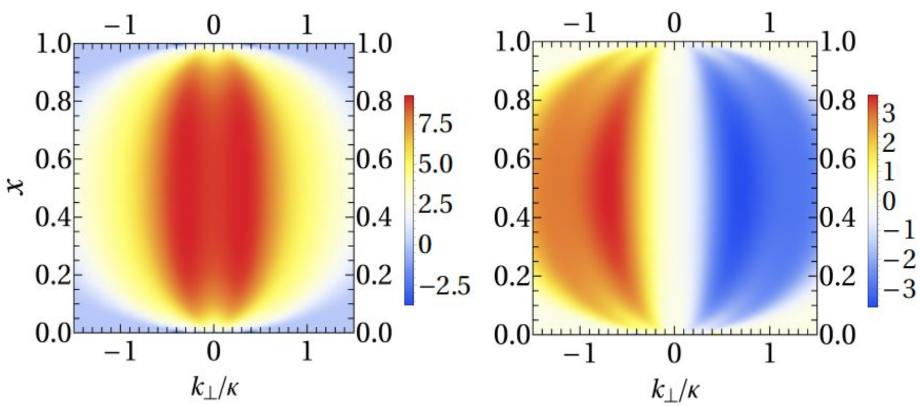

(a) π: $\psi_{\uparrow\downarrow-\downarrow\uparrow}(k_\perp, x)$ (b) π: $\psi_{\uparrow\uparrow}(k_\perp, x) = \psi_{\downarrow\downarrow}(k_\perp, x)$

LFWFs enable direct access to

- decay constants
- charge radius
- elastic form factors
- parton distribution functions
- QCD evolution

QCD evolutions

- <u>Parton distribution function (PDF):</u> we used **DGLAP equations** to evolve our initial PDF to experimental scale.

  [Dokshitzer, 1977]

- <u>Parton distribution amplitude (PDA)</u>: we used **ERBL equations** for the PDA evolution.

  [Lepage, 1980]

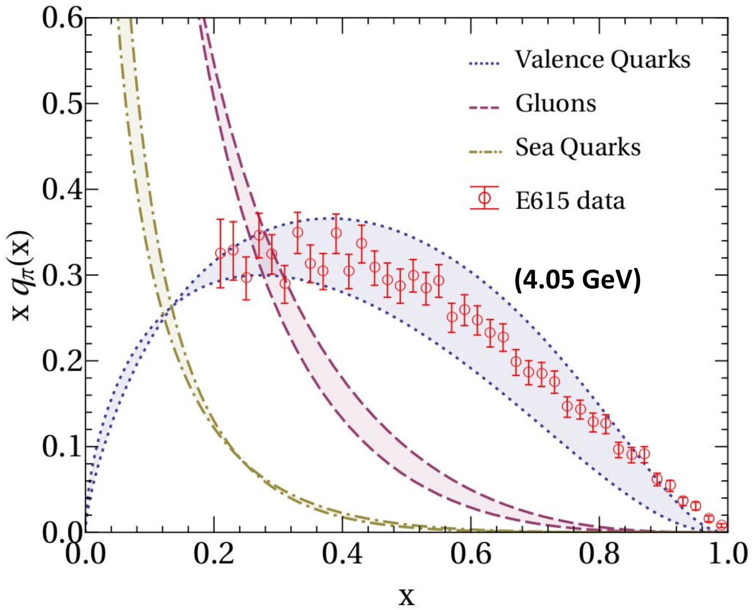

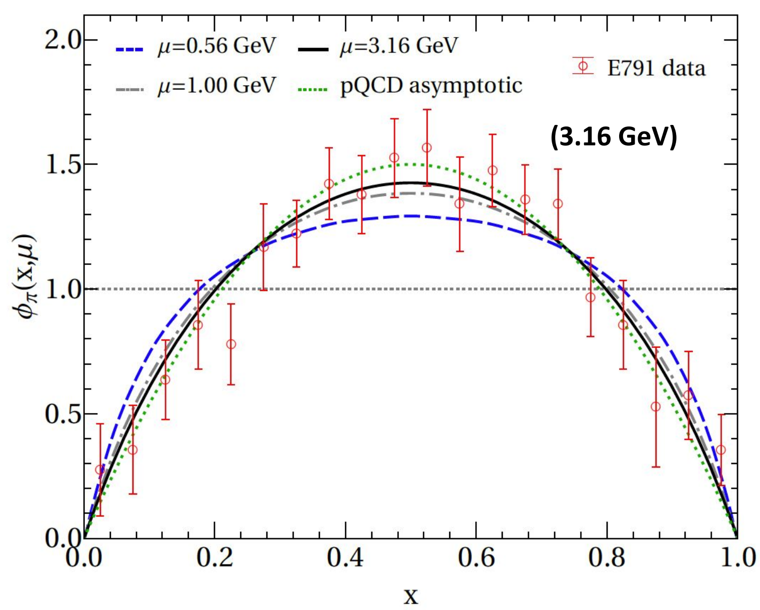

E615 data [Conway, 1989]

Initial scale $\mu_0 = 0.56$ GeV$\pm$ 5%

E791 data [Aitala, 2001]

Variational Quantum Eigensolvers (VQE)

[Peruzzo, 1304.3061]
[Nakanishi, 1810.09434]

VQE is directly inspired by the variational principle.

The core idea is to use a **parameterized unitary ansatz** (educated guess that produces the “trial wave function”) to obtain the lowest eigenvalue via continuous optimizations.

SSVQE:
Subspace-search VQE

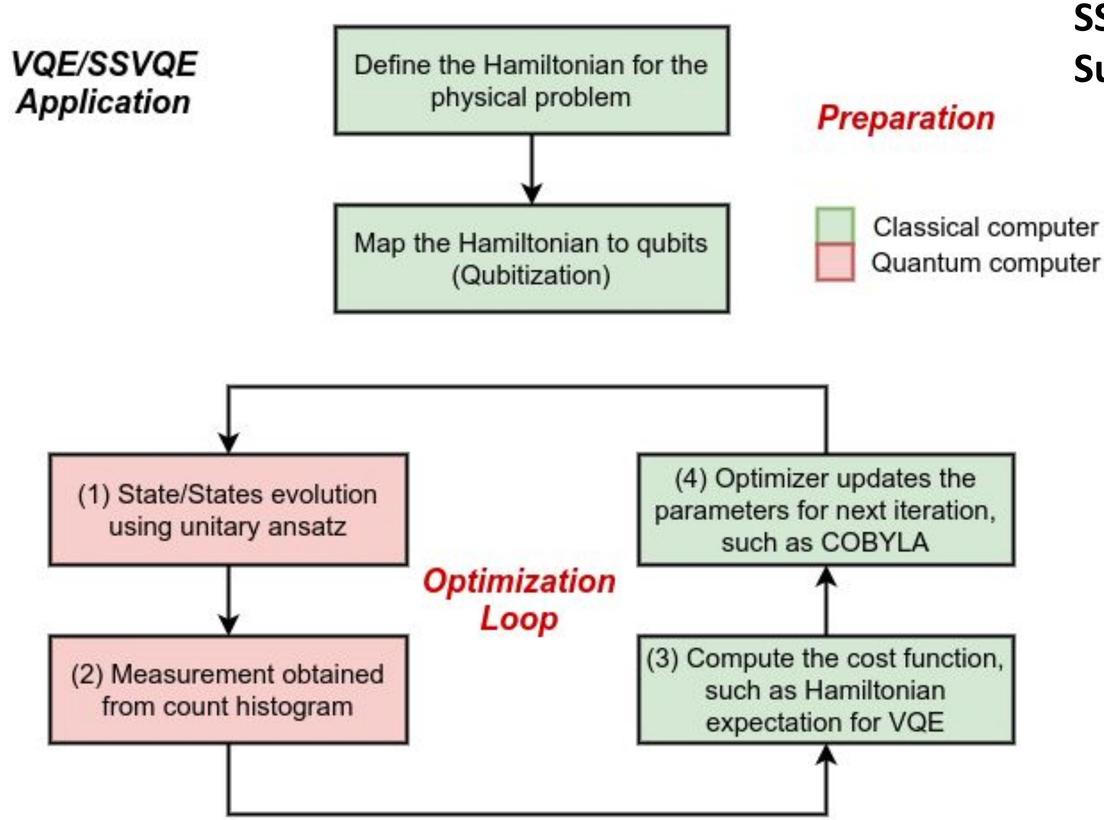

Adapting problem to quantum computers

For an initial application on quantum computers (or simulators), we truncate our basis functions at $(N_{\max}, L_{\max}) = (1,1)$ and $(N_{\max}, L_{\max}) = (4,1)$. [Qian, 2112.01927]

	N_{f}	$\alpha_{\mathrm{s}}(0)$	κ (MeV)	m_q (MeV)	$N_{\max}$	$L_{\max}$	Matrix dimension
$H_{\mathrm{eff}}^{(1,1)}$	3	0.89	560 ± 10	300 ± 10	1	1	4 by 4
$H_{\mathrm{eff}}^{(4,1)}$					4	1	16 by 16

- Encoding: **Jordan-Wigner** encoding $O(N)$, **compact** encoding $O(\log N)$

  $(N,N) = (2^n, 2^n) \to H_q = \sum_\alpha c_\alpha P_\alpha$ **Logarithmic scaling** [Jordan & Wigner (1928)] [Kreshchuk, 2002.04016]

- Variational ansatzes: **Unitary Coupled Cluster ansatz** and **Hardware Efficient heuristic ansatz**. [Barkoutsos, 1805.04340] [Kandala, 1704.05018]

- Algorithms: **VQE** for the ground state. **SSVQE** for the full spectroscopy. [Peruzzo, 1304.3061] [Nakanishi, 1810.09434]

With LFWF on qubits, additional physical observables (like decay constants) are computed *directly* on the quantum circuits.

Hamiltonian and basis encoding

Example of $N\mathrm{max} = L\mathrm{max} = 1$ (smallest Hamiltonian matrix) where matrix element corresponds to $(n,\ m,\ l,\ s,\ \bar{s})$ basis state,

$$H_{\mathrm{eff}}^{(1,1)} = \begin{pmatrix} 568487 & 0 & 25428 & 0 \\ 0 & 1700976 & 0 & -15767 \\ 25428 & 0 & 568487 & 0 \\ 0 & -15767 & 0 & 1700976 \end{pmatrix}$$

(All units in MeV^2)

	n	m	l	s	$\bar{s}$	Direct encoding	Compact encoding
1	0	0	0	1/2	-1/2	$\vert 0001\rangle$	$\vert 00\rangle$
2	0	0	0	-1/2	1/2	$\vert 0010\rangle$	$\vert 01\rangle$
3	0	0	1	1/2	-1/2	$\vert 0100\rangle$	$\vert 10\rangle$
4	0	0	1	-1/2	1/2	$\vert 1000\rangle$	$\vert 11\rangle$

From second quantization, the Hamiltonian can be written in terms of creation and annihilation operators,

$$\hat{H} = \hat{H}_1 + \hat{H}_2 + \cdots = \sum_{ij} h_{ij} \hat{a}_i^\dagger \hat{a}_j + \frac{1}{4} \sum_{ijkl} h_{ijkl} \hat{a}_i^\dagger \hat{a}_j^\dagger \hat{a}_k \hat{a}_l + \cdots$$

We focus only on the <u>single-body interactions</u> and identify h_{ij} as the Hamiltonian matrix elements.

Qubit encoding

Suppose H of dimension $(N,N)=(2^n,2^n)$ $\rightarrow H_q=\sum_\alpha c_\alpha P_\alpha$

[Jordan and Wigner (1928)]
[Seeley, 1208.5986]

1. **Direct encoding**: Jordan-Wigner (JW) encoding, basically map directly from using the 2 x 2 Pauli spin matrices $\sigma_k \in \{I_k, X_k, Y_k, Z_k\}$.

$$\boxed{O(N)}$$

$$\hat{a}_j^\dagger = \bigotimes_{i=1}^{j-1} Z_i \otimes \frac{X_j - iY_j}{2}$$

$$\hat{a}_j = \bigotimes_{i=1}^{j-1} Z_i \otimes \frac{X_j + iY_j}{2}$$

$$\begin{aligned} H^{(1,1)}_{\text{direct}} &= 2269462\,\mathrm{IIII} - 284243\,(\mathrm{ZIII}+\mathrm{IIZI}) \\ &- 850488\,(\mathrm{IZII}+\mathrm{IIIZ}) + 12714\,(\mathrm{XZXI}+\mathrm{YZYI}) \\ &- 7883\,(\mathrm{IXZX}+\mathrm{IYZY}), \end{aligned}$$

[Kreshchuk, 2002.04016]
[Nielson (2000)]

2. **Compact encoding**: utilize orthogonal basis formed by Pauli strings $P_\alpha = \otimes_{k=1}^n \sigma_k$ under trace, one can further reduce the N-by-N Hamiltonian (Hilbert-Schmidt inner product space)

$$\boxed{O(\log N) = O(n)}$$

$$H_q = \frac{1}{N}\sum_{\alpha=1}^{N^2} \mathrm{Tr}(P_\alpha H)\cdot P_\alpha$$

$$\begin{aligned} H^{(1,1)}_{\text{compact}} &= 1134731\,\mathrm{II} - 566245\,\mathrm{IZ} \\ &+ 4831\,\mathrm{XI} + 20598\,\mathrm{XZ} \end{aligned}$$

$$\mathrm{Tr}(P_j P_k) = 2^n \delta_{j,k} = N\delta_{j,k}$$

Variational ansatz $\hat{U}(\vec{\theta})$

Variational ansatz is an educated guess of the unitary circuit with parameters to be optimized in each iteration.

[Barkoutsos, 1805.04340]
[Romero, 1701.02691]

1. **Unitary coupled cluster (UCC)** ansatz

- motivated by coupled cluster methods

$$\hat{U}(\vec{\theta}) = e^{\hat{T}(\vec{\theta}) - \hat{T}^{\dagger}(\vec{\theta})}, \quad \hat{T}(\vec{\theta}) = \hat{T}_1(\vec{\theta}) = \sum_{\substack{r \in \mathrm{occ} \\ p \in \mathrm{virt}}} \theta_p^r \hat{a}_p^{\dagger} \hat{a}_r$$

$$\hat{U}(\vec{\theta}) = e^{i \sum_{\alpha} c_{\alpha} P_{\alpha}}$$

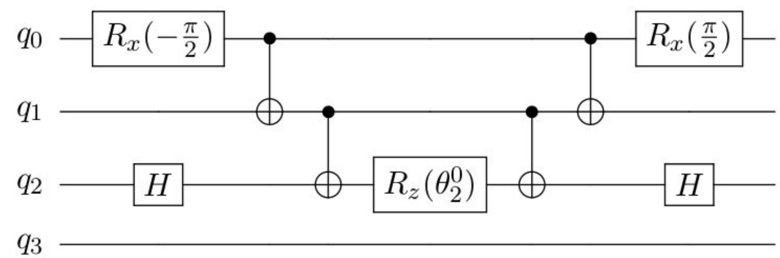

UCC(Single) circuit for $e^{i\,\theta_3^0\,\hat{a}_3^{\dagger}\,\hat{a}_0}$

2. **Hardware efficient (HE)** ansatz [Kandala, 1704.05018]

- **heuristic** ansatz
- consists of alternating single-qubit rotations and entangling blocks (repetition layers)
- proven to work for general problems

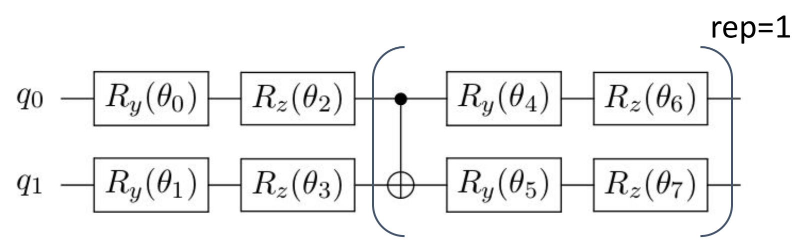

EfficientSU2 ansatz with 1 repetition layer

[Qiskit 0.32.1 library]

Optimization algorithms

❖ **<u>Variational Quantum Eigensolver (VQE)</u>** algorithm finds <u>ground state</u>

[Peruzzo, 1304.3061]

Initial state $\|\psi\rangle$	→	Unitary evolution $\|\psi(\vec{\theta})\rangle = \hat{U}(\vec{\theta})\,\|\psi\rangle$	→	Measure & compute cost function $C(\vec{\theta}) = \langle\psi(\vec{\theta})\|\,\hat{H}\,\|\psi(\vec{\theta})\rangle$

❖ **<u>Subspace-search VQE (SSVQE)</u>** algorithm finds <u>excited states</u>

In particular, **Weighted SSVQE** for up to *k*-th excited states [Nakanishi, 1810.09434]

Set of orthogonal states $\{\|\psi_i\rangle\}_{i=0}^{k}$	→	Evolution for each state $\|\psi_i(\vec{\theta})\rangle = \hat{U}(\vec{\theta})\,\|\psi_i\rangle$	→	Measure & compute cost function $C_{\vec{\omega}}(\vec{\theta}) = \vec{\omega}\cdot\vec{E}$

$$\vec{E} = (E_0, E_1, \cdots, E_k) \qquad E_i = \langle\psi_i(\vec{\theta})|\hat{H}|\psi_i(\vec{\theta})\rangle$$

$\vec{\omega}$ is a strictly decreasing weight vector prioritizing lower-lying states

For example: $C_{\vec{\omega}}(\vec{\theta}) = E_0 + 0.5E_1 + 0.25E_2, \quad \vec{\omega} = (1, 0.5, 0.25)$

Results: VQE $(N_{\max}, L_{\max}) = (1, 1)$

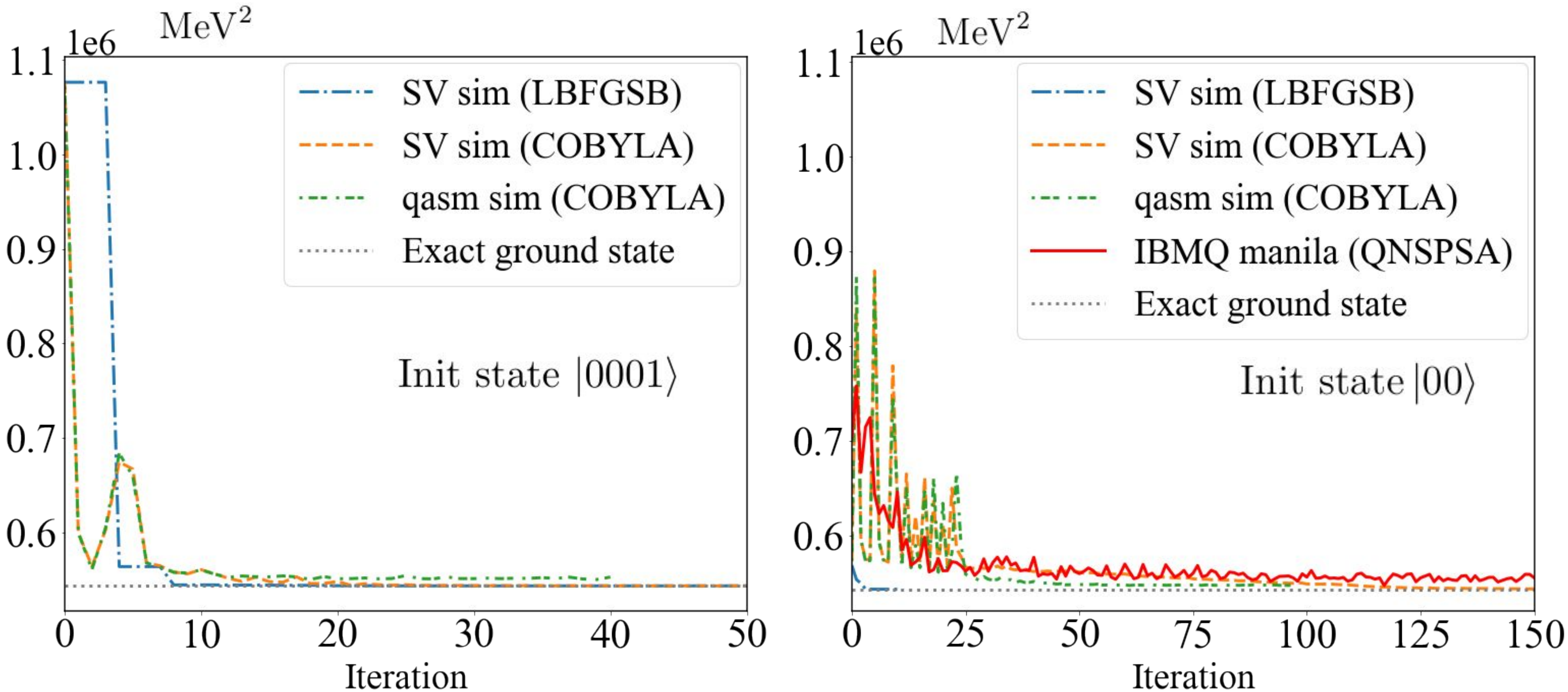

(a) Direct encoding with VQE

(b) Compact encoding with VQE

- Ansatz: UCCS ansatz, 50 gates — HE ansatz, 9 gates (1 layer)
- IBM simulators + backends:

- statevector (SV) simulator (noise-free exact simulation)
- qasm simulator (sampling noise from 8192 shots per measurement)
- IBMQ manila (5 Qubits, 32 QV, 2.8K CLOPS, 2e-2% readout error, 8192 shots per measurement)

[Qiskit 0.32.1 library]

Results: SSVQE $(N_{\max}, L_{\max}) = (1, 1)$

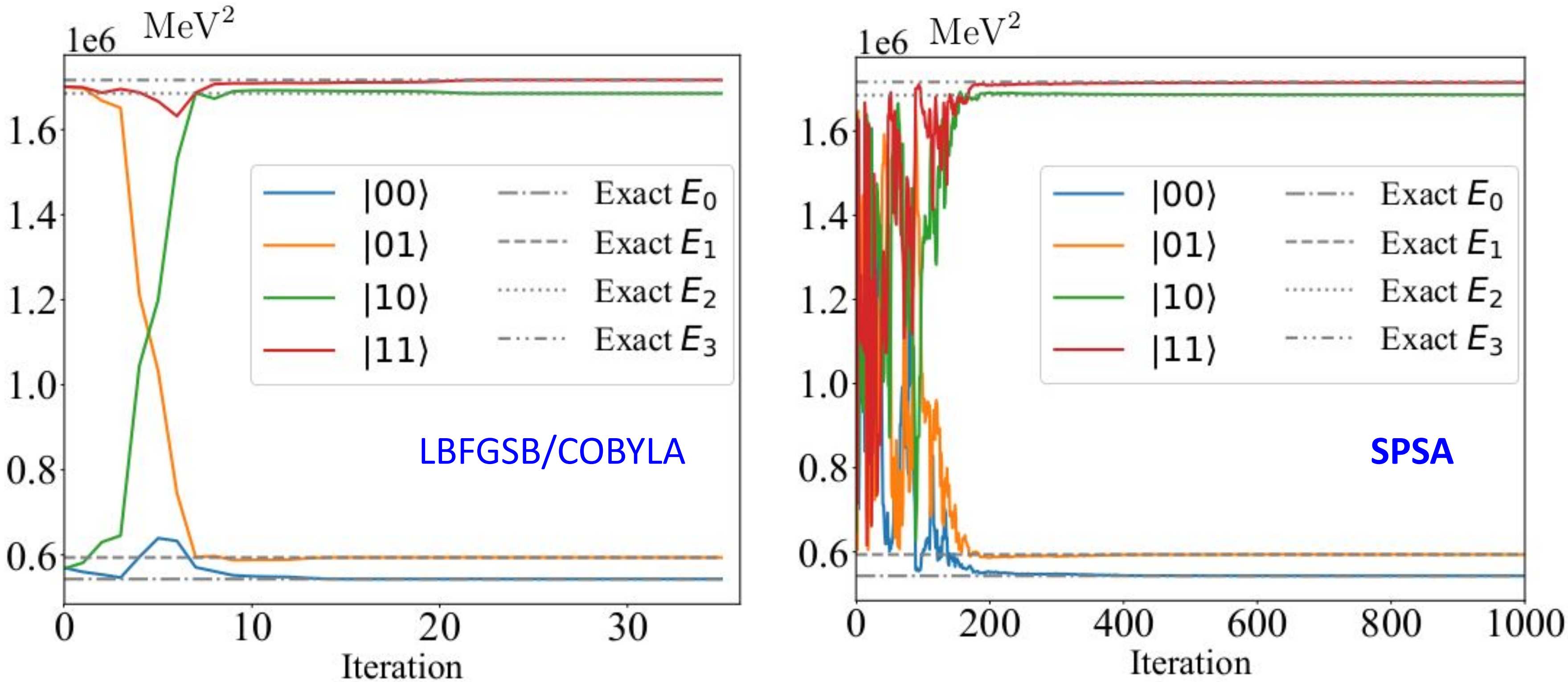

(a) SSVQE with statevector simulator

(b) SSVQE with qasm simulator

- Both use <u>compact encoding with HE ansatz</u> (2 repetition layers, 12 params)
- Cost function:

$$1.0 \cdot E_{|00\rangle} + 0.5 \cdot E_{|01\rangle} + 0.25 \cdot E_{|10\rangle} + 0.125 \cdot E_{|11\rangle}$$

- Note:
  Spectrum always <u>emerge in accordance</u> with the specified weight order.

Results: SSVQE $(N_{\max}, L_{\max}) = (4, 1)$

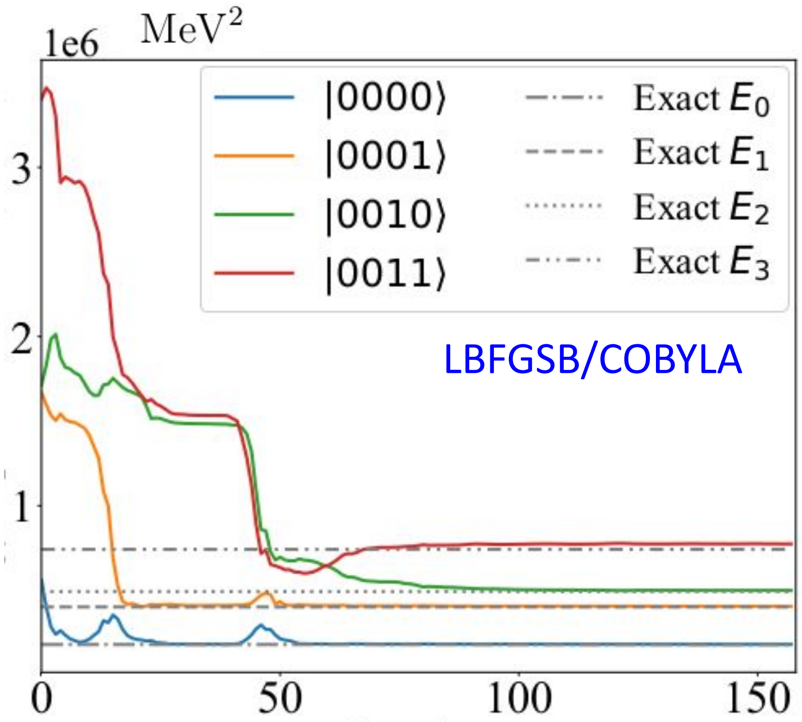

(a) SSVQE with statevector simulator

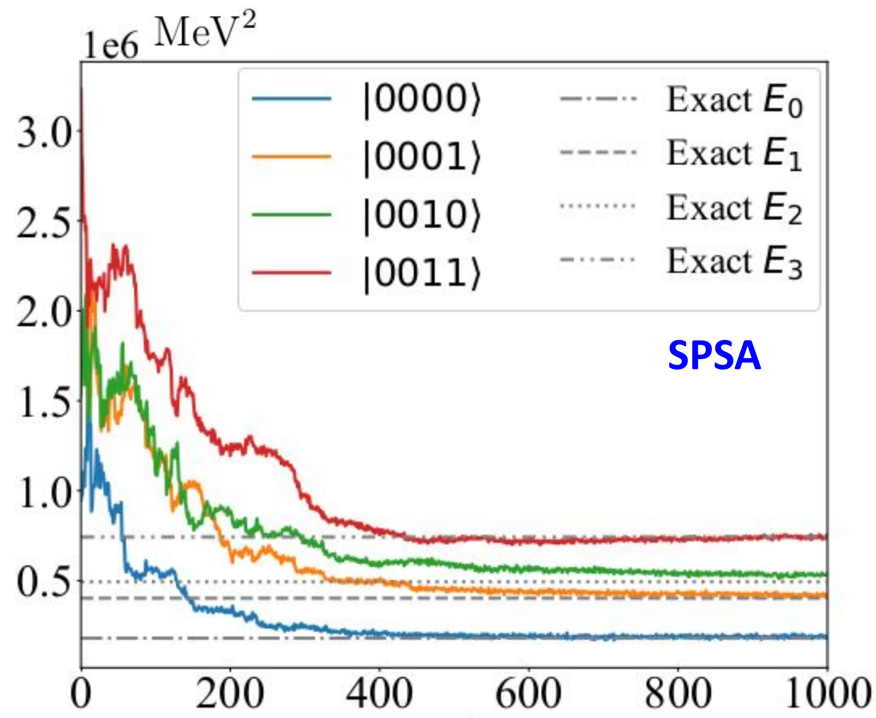

(b) SSVQE with qasm simulator

- Low-lying spectrum (lowest 4 states instead of 16 possible states)
- Both use <u>compact encoding with HE ansatz</u> (6 repetition layer, 53 params)

Results: decay constants

Decay constants are defined as vacuum-to-hadron matrix element of the quark current operator. In BLFQ basis, we write the decay constants as:

$$f_{\mathrm{P,V}} = 2\sqrt{2N_c}\int_0^1 \frac{\mathrm{d}x}{2\sqrt{x(1-x)}}\int\frac{\mathrm{d}^2\boldsymbol{k}_\perp}{(2\pi)^3}\psi^{(m_j=0)}_{\uparrow\downarrow\mp\downarrow\uparrow}(x,\boldsymbol{k}_\perp)$$

$$\equiv \frac{\kappa\sqrt{N_c}}{\pi}\sum_{nl}(-1)^n C_l(m_q,\kappa)\left(\tilde{\psi}^{(m_j=0)}_{\uparrow\downarrow}(n,0,l) \mp \tilde{\psi}^{(m_j=0)}_{\downarrow\uparrow}(n,0,l)\right)$$

[Li, 1704.06968]

In the VQE/SSVQE, the light-front wave function (LFWF) is encoded on the qubits. One can **directly** compute observables such as decay constants on the quantum circuit:

$$f_{\mathrm{P,V}} \propto \ |\langle \nu_{\mathrm{P,V}}|\psi(\vec{\theta})\rangle| = \sqrt{\langle\psi(\vec{\theta})|(|\nu_{P,V}\rangle\langle\nu_{P,V}|)|\psi(\vec{\theta})\rangle}$$

For example, in $(N_{\mathrm{max}}, L_{\mathrm{max}}) = (1,1)$

$$\nu^{(1,1)}_{\mathrm{P}} = (1,-1,0,0)$$
$$\nu^{(1,1)}_{\mathrm{V}} = (1,1,0,0)$$

$$\longrightarrow \quad |\nu^{(1,1)}_{P,V}\rangle\langle\nu^{(1,1)}_{P,V}|_q = 0.5\,(II \mp IX + ZI \pm ZX)$$

Results: decay constants

Summary of decay constants for the lowest two states (π and ρ mesons). Experimental decay constants are around 130 MeV and 216 MeV, respectively.

[Zyla, 2020]

$N_{\max}$	$L_{\max}$	Decay constants	Exact result (MeV)	SV sim (MeV)	qasm sim (MeV)
1	1	f_π	178.18	178.18	178.17 ± 1.97
		f_ρ	178.18	178.18	178.17 ± 1.97
4	1	f_π	193.71	193.32	194.28 ± 15.49
		f_ρ	231.00	232.93	225.72 ± 13.44

Uncertainty (sampling error) in qasm simulator results from measurements of 8192 shots.

Results: parton distribution functions

Parton distribution functions (PDFs) is the probability of finding a particle with longitudinal momentum fraction x under some factorization scale related to experimental conditions,

$$q(x;\mu) = \frac{1}{x(1-x)}\sum_{s\bar{s}}\int \frac{\mathrm{d}^2\boldsymbol{k}_\perp}{2(2\pi)^3}|\psi_{s\bar{s}}^{(m_j=0)}(x,\boldsymbol{k}_\perp)|^2$$

[Li, 1704.06968]

$$\equiv \frac{1}{4\pi}\sum_{s\bar{s}}\sum_{nm}\sum_{l\bar{l}}\tilde{\psi}_{s\bar{s}}^{*(m_j=0)}(n,m,\bar{l})\tilde{\psi}_{s\bar{s}}^{(m_j=0)}(n,m,l)\chi_l(x)\chi_{\bar{l}}(x)$$

Using projection operators, one can **directly** compute the PDF on quantum computers as well. Note: PDF operator on qubits depends on x.

$$q(x) = \sum_{s\bar{s}}\sum_{nm}\sum_{l\bar{l}}\langle\psi(\vec{\theta})|\,\hat{O}_{\mathrm{pdf}}(x)\,|\psi(\vec{\theta})\rangle$$

Qubitized operators:

$$\hat{O}_{\mathrm{pdf}}(x) = \hat{U}_{\mathrm{p}}(s,\bar{s},n,m,\bar{l})^\dagger\hat{U}_{\mathrm{p}}(s,\bar{s},n,m,l)\chi_l(x)\chi_{\bar{l}}(x)/4\pi$$

$$\hat{O}_{\mathrm{pdf}}^{(1,1)}(0.5)_q = 1.30\,II - 1.29\,IX - 0.18\,IZ, \qquad \hat{O}_{\mathrm{pdf}}^{(1,1)}(0.25)_q = 0.78\left(II + IZ\right)$$

Results: parton distribution functions

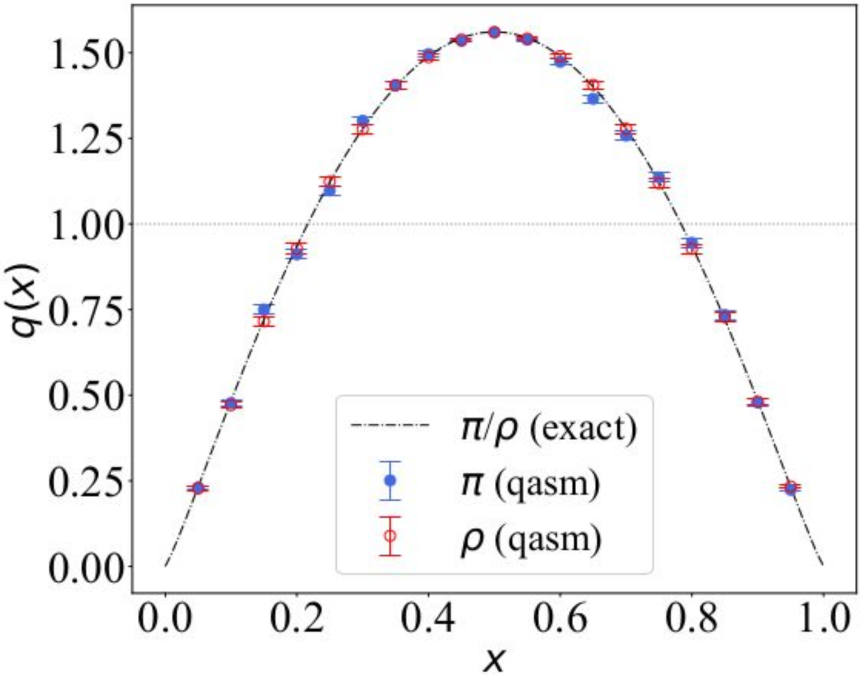

(a) PDFs at $N_{\max} = L_{\max} = 1$

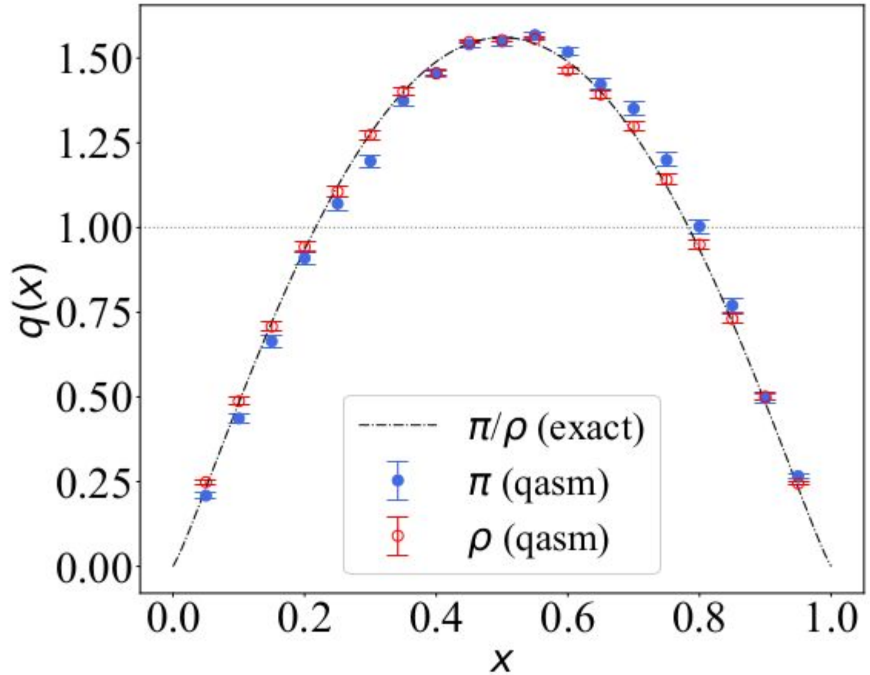

(b) PDFs at $N_{\max} = 4, L_{\max} = 1$

- In both basis truncations, the PDFs for lowest two states are comparable due to the lack of longitudinal excitations.
- For $(N_{\max}, L_{\max}) = (1, 1)$, qasm results agree with exact calculations.
- For $(N_{\max}, L_{\max}) = (4, 1)$, PDF is rescaled due to lack of normality of the PDF/LFWF at this cutoff.

Radiative transitions (Preliminary)

The electromagnetic transition between two hadron states is governed by the hadron matrix element, which is key to calculating the transition form factor & decay width (probe the internal structure of QCD bound state):

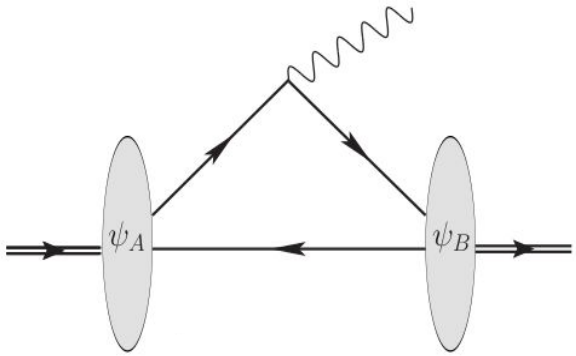

[M Li, 1803.11519]

$$I^{\mu}_{m'_j, m_j} = \langle \psi_B(p', j', m'_j) | J^{\mu}(x) | \psi_A(p, j, m_j) \rangle$$

For example, a physical process between a vector meson (V) and a pseudoscalar (P), $\mathrm{V} \to \mathrm{P} + \gamma$

The SSVQE approach allows one to compute any transition amplitude by using a <u>superposition</u> of the incoming and outgoing meson states.

[Nakanishi, 1810.09434]

$$A = \langle \psi_i(\vec{\theta}) | \hat{A} | \psi_j(\vec{\theta}) \rangle = \langle \psi_i | U^{\dagger}(\vec{\theta}) \hat{A} U(\vec{\theta}) | \psi_j \rangle$$

$$\begin{aligned} \mathrm{Re}(A) = {} & \langle \psi_{ij}^{+x} | U^{\dagger}(\vec{\theta}) \hat{A} U(\vec{\theta}) | \psi_{ij}^{+x} \rangle \\ & - \frac{1}{2} \Big(\langle \psi_i | U^{\dagger}(\vec{\theta}) \hat{A} U(\vec{\theta}) | \psi_i \rangle + \langle \psi_j | U^{\dagger}(\vec{\theta}) \hat{A} U(\vec{\theta}) | \psi_j \rangle \Big) \end{aligned}$$

$$\boxed{|\psi_{ij}^{+x}\rangle = \frac{1}{\sqrt{2}} (|\psi_i\rangle + |\psi_j\rangle)}$$

$$\begin{aligned} \mathrm{Im}(A) = {} & \langle \psi_{ij}^{+y} | U^{\dagger}(\vec{\theta}) \hat{A} U(\vec{\theta}) | \psi_{ij}^{+y} \rangle \\ & - \frac{1}{2} \Big(\langle \psi_i | U^{\dagger}(\vec{\theta}) \hat{A} U(\vec{\theta}) | \psi_i \rangle + \langle \psi_j | U^{\dagger}(\vec{\theta}) \hat{A} U(\vec{\theta}) | \psi_j \rangle \Big) \end{aligned}$$

$$\boxed{|\psi_{ij}^{+y}\rangle = \frac{1}{\sqrt{2}} (|\psi_i\rangle + i\, |\psi_j\rangle)}$$

Radiative transitions (Preliminary)

<u>Initial quantum circuits</u> for calculating $\mathrm{Re}(A)$ or $\mathrm{Im}(A)$ can be constructed with only X, H, S, CX gates. Switching H with S-H-S gates to calculate $\mathrm{Im}(A)$.

states	qubits	circuit
$\frac{1}{\sqrt{2}}(\psi_0+\psi_1)$	$\|0+\rangle$	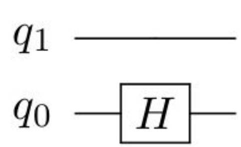
$\frac{1}{\sqrt{2}}(\psi_0+\psi_2)$	$\|+0\rangle$	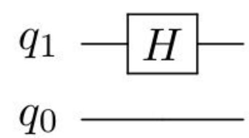
$\frac{1}{\sqrt{2}}(\psi_0+\psi_3)$	$\mathrm{CX}(0,1)\,\|0+\rangle$	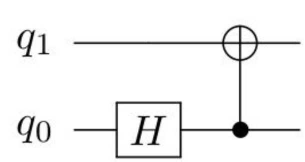
$\frac{1}{\sqrt{2}}(\psi_1+\psi_2)$	$\mathrm{CX}(1,0)\,\|+1\rangle$	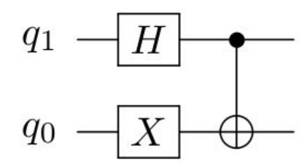
$\frac{1}{\sqrt{2}}(\psi_1+\psi_3)$	$\|+1\rangle$	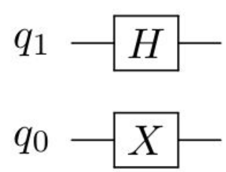
$\frac{1}{\sqrt{2}}(\psi_2+\psi_3)$	$\|1+\rangle$	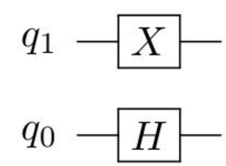

Summary and outlook

We presented two promising quantum computing approaches, VQE and SSVQE, to find meson spectroscopy and observables on the light front for the light meson system.

Basis light-front quantization approach (BLFQ) works well with the VQE and SSVQE approaches.

Future plans:

- Optimize the VQE and SSVQE programs to solve the original Hamiltonian and compute on real quantum backends.
  $N_{\max} = 8,\ L_{\max} = 1$ => (32, 32) Hamiltonian => 5 qubits
  $N_{\max} = 8,\ L_{\max} = 3$ => (64, 64) Hamiltonian => 6 qubits

  Logarithmic scaling
  (compact encoding)

- Calculations on transition matrix element of an operator using SSVQE approach. Take advantage of **quantum superposition**!

- Investigation into other **many-body** QCD bound state problems.

Backup slides

Light-front dynamics

Light-front quantum field theory is quantized on: $x^+ = 0$

[Review Papers: Burkardt 1996, Brodsky 1998, Hiller 2016]

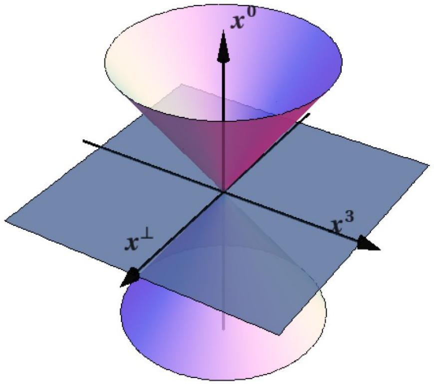

instant form ($t = x^0$)

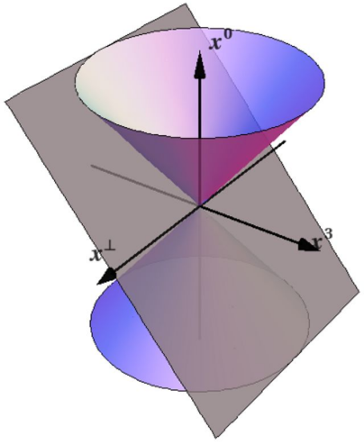

front form ($x^+ = x^0 + x^3$)

[Dirac, 1949]

- ❖ Simplifies the dispersion relation

$$P^0 = \sqrt{m^2 + \vec{P}} \quad \Rightarrow \quad P^- = (m^2 + \mathbf{P}_\perp^2)/P^+$$

- ❖ One more kinematical variable
- ❖ Light-front vacuum is trivial (we ignore zero mode)

LF time: $x^+ = x^0 + x^3$ LF energy: $P^- = P^0 - P^3$

LF longitudinal momentum: $P^+ = P^0 + P^3$ LF transverse momentum: $\mathbf{P} \equiv \vec{P}^\perp = (P^1, P^2)$

Light mesons Hamiltonian in detail

Light-front Hamiltonian in $|q\bar{q}\rangle$:

$$H_{\mathrm{eff},\gamma_5} = \overbrace{\underbrace{\frac{\mathbf{k}_\perp^2 + m_q^2}{x} + \frac{\mathbf{k}_\perp^2 + m_{\bar{q}}^2}{1-x}}_{\text{LF kinetic energy}} + \underbrace{\kappa^4 x(1-x)\mathbf{r}_\perp^2 - \frac{\kappa^4}{(m_q+m_{\bar{q}})^2}\frac{\partial}{\partial x}\left(x(1-x)\frac{\partial}{\partial x}\right)}_{\text{confinement}} + V_g}^{H_{\mathrm{eff}}} + H_{\gamma_5}$$

$$\text{where } x = p_q^+/P^+, \mathbf{k}_\perp = \mathbf{p}_{q\perp} - x\mathbf{P}_\perp, \mathbf{r}_\perp = \mathbf{r}_{q\perp} - \mathbf{r}_{\bar{q}\perp}$$

1. Light-front Kinetic energy
2. Confinement:
   (a) Transverse holographic confinement [Brodsky, 2015]
   (b) Longitudinal confinement [Li, 2016]
3. One-gluon exchange with running coupling [Krautgartner, 1992]

$$V_g = -\frac{4}{3}\frac{4\pi\alpha_s(Q^2)}{Q^2}\bar{u}_{s'}(\mathbf{k}'_\perp, x')\gamma_\mu u_s(\mathbf{k}_\perp, x)\bar{v}_{\bar{s}}(-\mathbf{k}_\perp, 1-x)\gamma^\mu v_{\bar{s}'}(-\mathbf{k}'_\perp, 1-x')$$

4. Point-like pseudoscalar interaction [Inspired by Jia, 2019 & Mannheim, 2017]

$$\mathcal{H}_{\gamma_5} = \lambda\bar{\psi}(x)\gamma^5\psi(x)\bar{\psi}(x)\gamma^5\psi(x)$$

General approach to the entire light meson sector with simplification of isospin and charge

Basis functions in detail

relative-particle coordinate

- Basis functions [Li, 2016; 2017]

$$\psi_{s\bar{s}/h}(\mathbf{k}_\perp, x) = \sum_{n,m,l} \psi_h(n,m,l,s,\bar{s})\phi(\mathbf{k}_\perp/\sqrt{x(1-x)})\chi_l(x)$$

(2D HO functions)

- Transverse: $$\phi_{nm}(\mathbf{q}_\perp) = \frac{1}{\kappa}\sqrt{\frac{4\pi n!}{(n+|m|)!}}\left(\frac{q_\perp}{\kappa}\right)^{|m|} e^{-\frac{1}{2}q_\perp^2/\kappa^2} L_n^{|m|}(q_\perp^2/\kappa^2)e^{im\theta_q}$$

- Longitudinal: $$\chi_l(x;\alpha,\beta) = \sqrt{4\pi(2l+\alpha+\beta+1)}\sqrt{\frac{\Gamma(l+1)\Gamma(l+\alpha+\beta+1)}{\Gamma(l+\alpha+1)(\Gamma(l+\beta+1)}}x^{\frac{\beta}{2}}(1-x)^{\frac{\alpha}{2}}P_l^{(\alpha,\beta)}(2x-1)$$

(Jacobi polynomials)

$$\text{where } \alpha = 2m_{\bar{q}}(m_q+m_{\bar{q}})/\kappa^2, \beta = 2m_q(m_q+m_{\bar{q}})/\kappa^2$$

- Basis truncations $\quad 2n+|m|+1 \le N_{\max} \qquad l \le L_{\max}$

- Cutoff and resolution $\quad \Lambda_{\text{uv}} \approx \kappa\sqrt{N_{\max}} \qquad \lambda_{\text{IR}} \approx \kappa/\sqrt{N_{\max}} \qquad \Delta x \approx L_{\max}^{-1}$

This model serves as first step to the light meson sector with BLFQ, and provides access to the full spectroscopy.

Spectroscopy

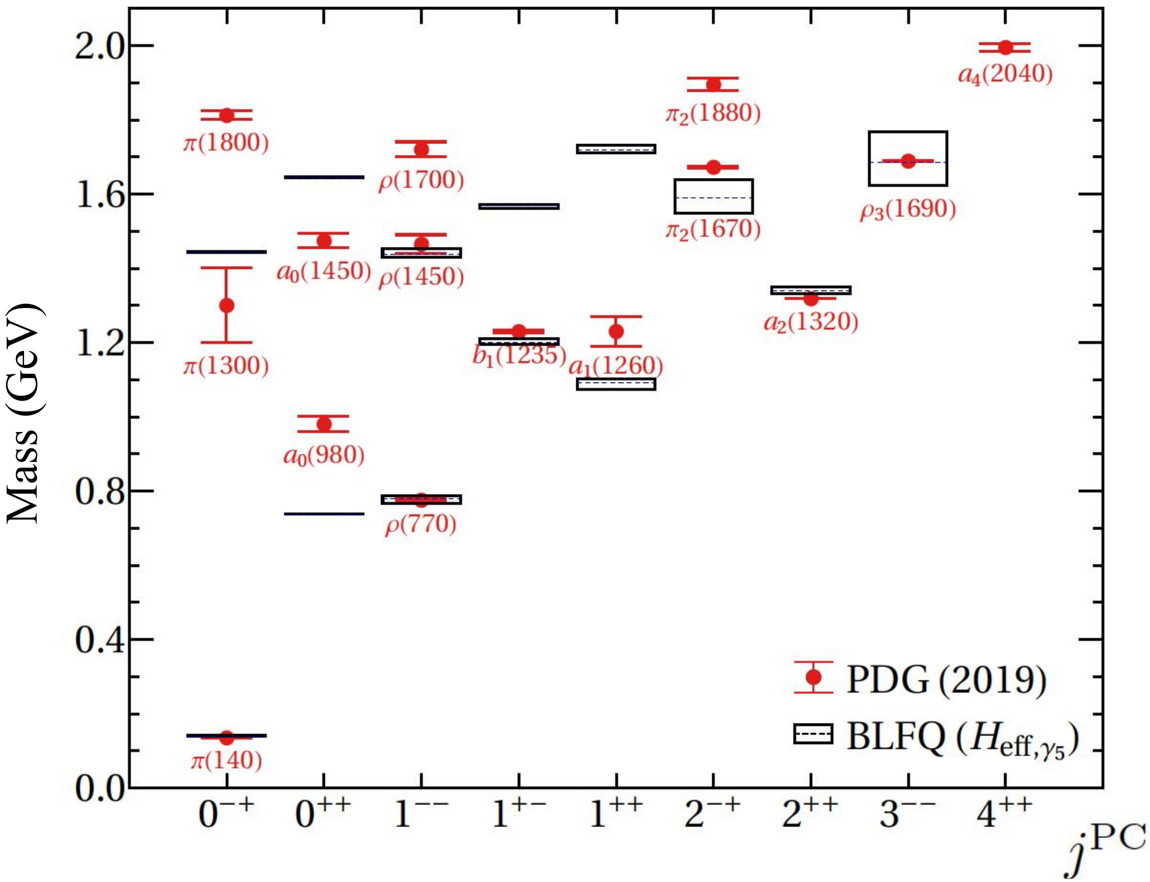

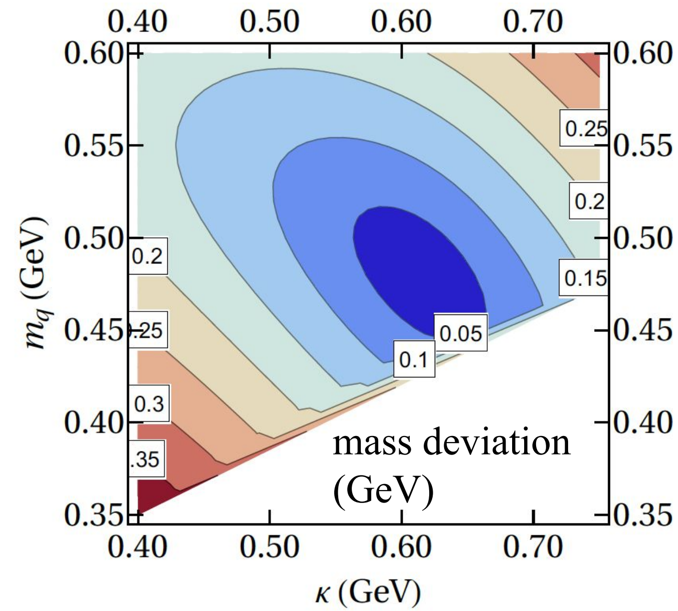

Fitted masses (in asterisk):
$\rho(770)$, ρ (1450), π (140)

	N_f	$\alpha_s(0)$	κ (MeV)	$m_q = m_{\bar{q}}$ (MeV)	N_{exp}	N_{max}	L_{max}	λ (GeV^{-2})	r.m.s. (MeV)
H_{eff}	3	0.89	610 (5) *	480 (5) *	11	8	24	-	127
H_{eff,γ_5}								0.56(1) *	111

Root mean square (r.m.s.) measures the overall discrepancy between PDG and BLFQ for the 11 identified states.

[Qian, 2005.13806]

Spectroscopy comparison

Comparison with experimental data and other model calculations (in GeV). Fitted masses are labeled with red asterisks.

	j	P	C	PDG	AdS/QCD	BSE	BLFQ (H_{eff,γ_5}) (This work)
$\pi(140)$	0	$-$	$+$	0.14	0.14 *	0.14 (0.14) *	0.14 *
$\rho(770)$	1	$-$	$-$	0.78	0.78	0.76 (0.74)	0.78 *
$a_0(980)$	0	$+$	$+$	0.98	0.78	0.64 (1.1)	0.74
$b_1(1235)$	1	$+$	$-$	1.23	1.09	0.85 (1.3)	1.20
$a_1(1260)$	1	$+$	$+$	1.23	1.09	0.97 (1.3)	1.09
$\pi(1300)$	0	$-$	$+$	1.30	1.09	1.10	1.44
$a_2(1320)$	2	$+$	$+$	1.32	1.33	1.16	1.34
$\rho(1450)$	1	$-$	$+$	1.45	1.33	1.02	1.44 *
$a_0(1450)$	0	$+$	$+$	1.47	1.33	1.27	1.65
$\pi_2(1670)$	2	$-$	$+$	1.67	1.53	1.23	1.59
$\rho_3(1690)$	3	$-$	$+$	1.69	1.71	1.54	1.69
				(r.m.s.)	127 MeV	275 (220) MeV	111 MeV

PDG [Tanabashi, 2018]
AdS (anti-de Sitter space) /QCD [Brodsky, 2015]
BSE (Bethe-Salpeter equation) [Fischer, 2014; Williams, 2016]

[Qian, 2005.13806]

Light-Front Wavefunction (LFWF)

LFWFs (as eigenvectors) are also obtained. This is a key advantage of Hamiltonian formalism, which enables us to compute physical observables.

[Qian, 2005.13806]

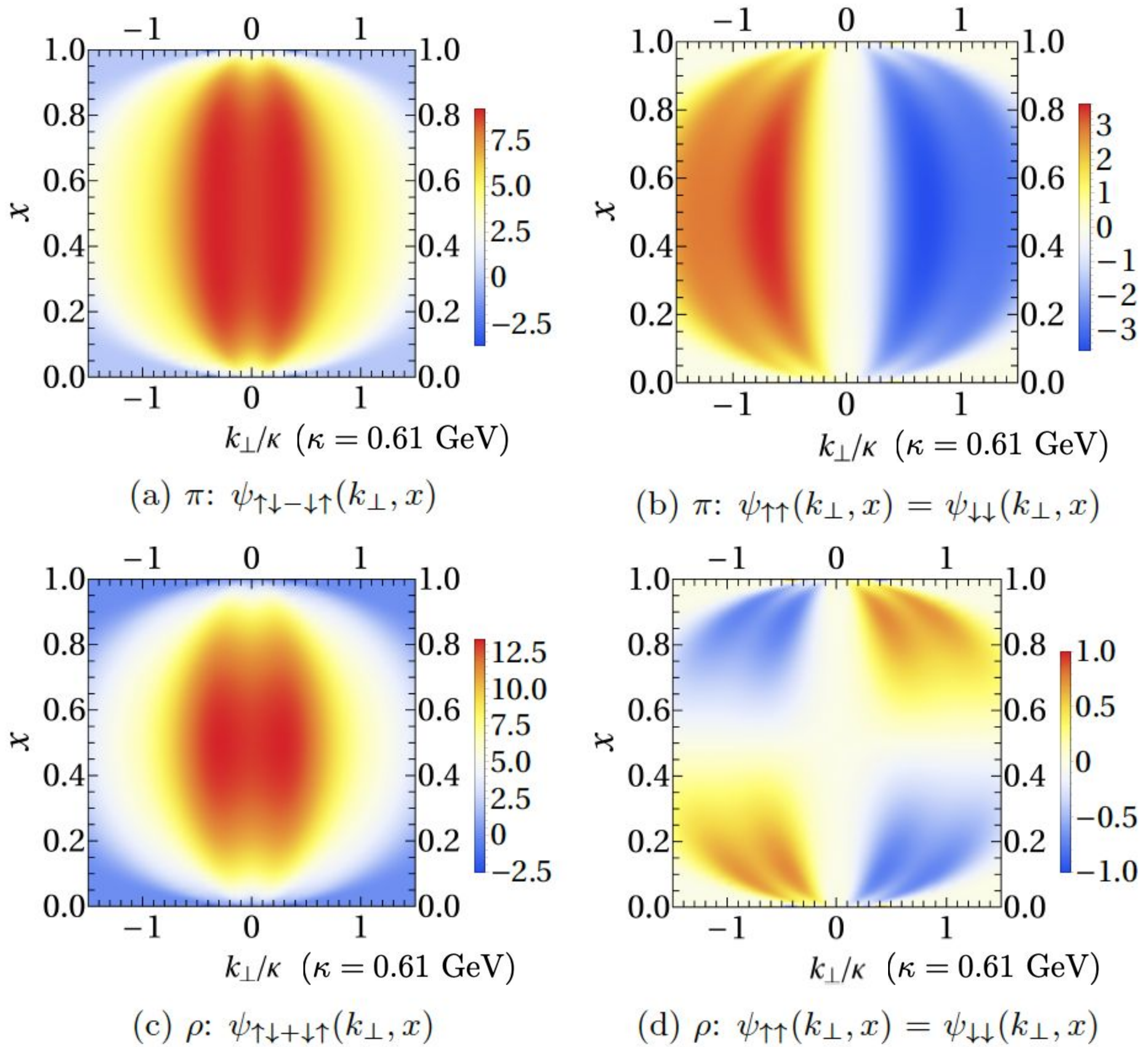

(a) π: $\psi_{\uparrow\downarrow-\downarrow\uparrow}(k_\perp, x)$

(b) π: $\psi_{\uparrow\uparrow}(k_\perp, x) = \psi_{\downarrow\downarrow}(k_\perp, x)$

(c) ρ: $\psi_{\uparrow\downarrow+\downarrow\uparrow}(k_\perp, x)$

(d) ρ: $\psi_{\uparrow\uparrow}(k_\perp, x) = \psi_{\downarrow\downarrow}(k_\perp, x)$

Comparison with other systems. Dominant wavefunctions(singlet) for pseudoscalar mesons from heavy to light systems:

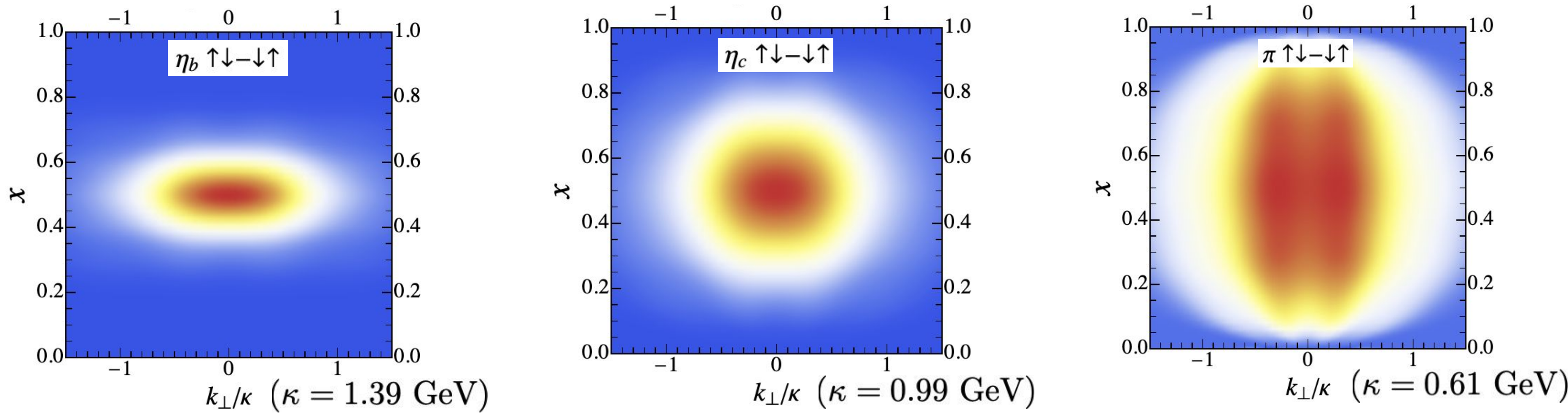

[Y. Li, 1704.06968]
[Qian, 2005.13806]

Comparison of LFWF spin components:

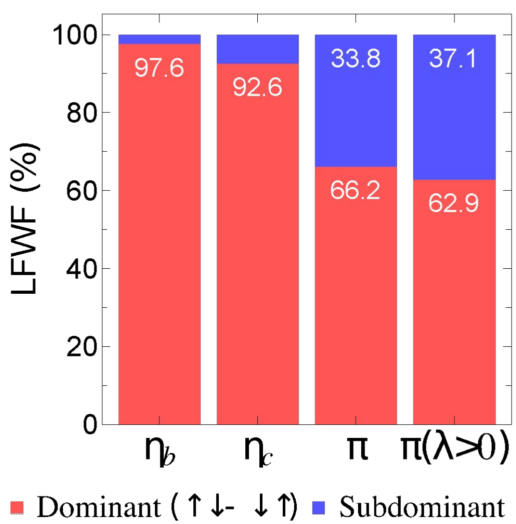

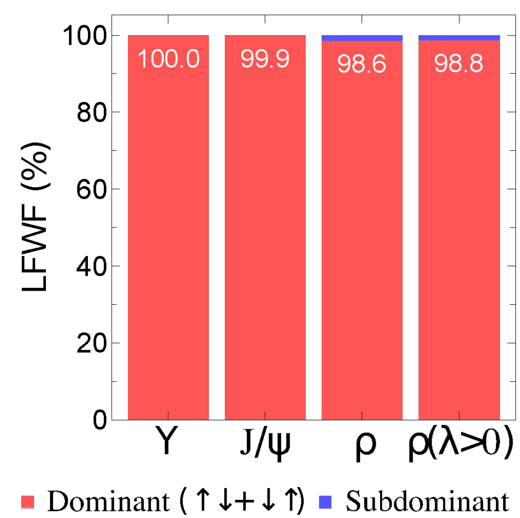

Quantum circuit basics

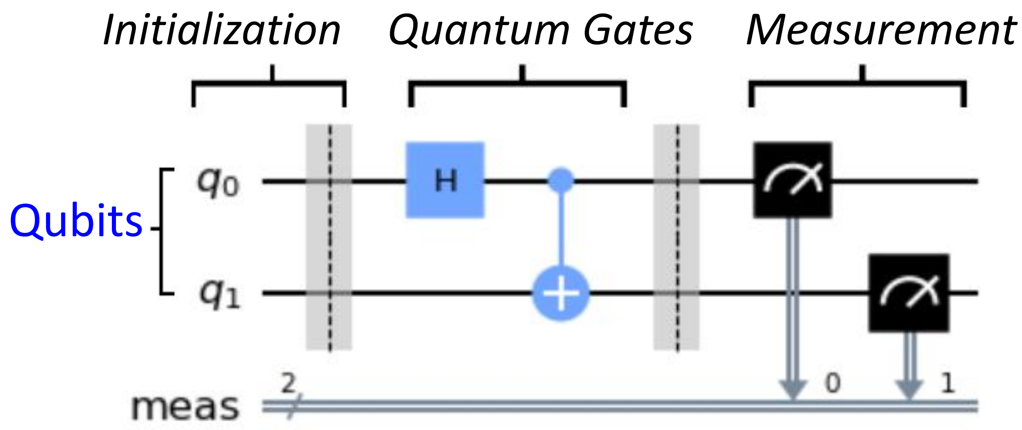

Quantum circuit

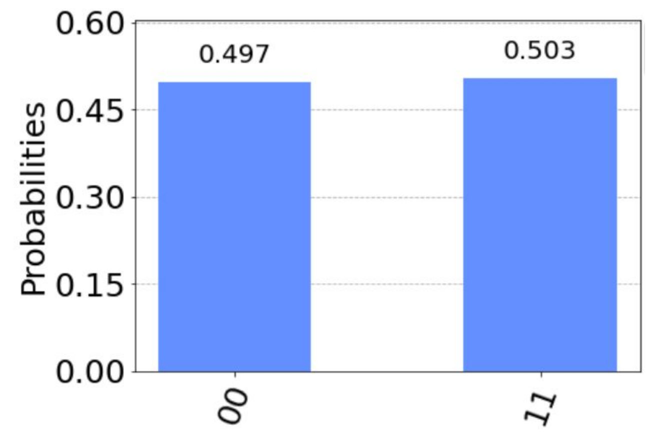

Outcome

- Each horizontal line represents the evolution of a qubit (from left to right)
- Each measurement collapses the wave function and we obtain either 0 or 1 in the computation basis
- In practice, measurements are statistical outcomes by running the same circuit repeatedly for thousands of times (or shots)
- Finally, statistical outcomes lead to find the associated expectation value.

Optimizers

Optimizers (on classical computers) aim to minimize the loss functions and updates the parameter for next iteration.

- **COBYLA**: constrained optimization, derivative-free
- **LBFGSB**: quasi-Newton method, derivative-based
- **SPSA**: Simultaneous Perturbation Stochastic Approximation; can handle measurement uncertainty [diagram from Pennylane]
- **QNSPSA**: Quantum Natural SPSA; improve SPSA by sampling natural gradients; significant speed up

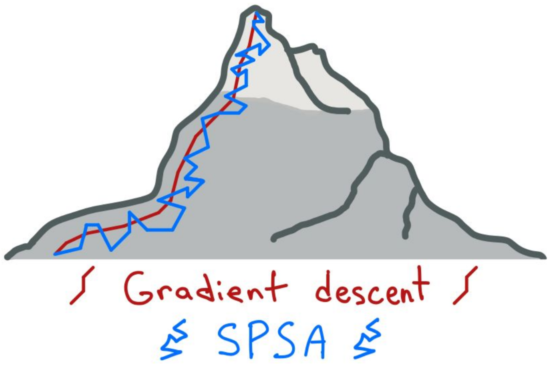

More optimizers at
scipy.optimize.minimize
qiskit.algorithms.optimizers

Detailed statistics of VQE results

Simulator	Encoding	Optimizer	Ground state energy (MeV^2)	Iterations
SV	Direct	LBFGSB	543059 (0%)	60
	Direct	COBYLA	543059 (0%)	90
	Compact	LBFGSB	543059 (0%)	11
	Compact	COBYLA	543059 (0%)	344
qasm	Direct	COBYLA	552344 ± 996 (1.53%)	41
	Direct	SPSA	545767 ± 152 (0.47%)	1051
	Compact	COBYLA	547405 ± 211 (0.76%)	99
	Compact	SPSA	543065 ± 6 (0%)	1551
Exact solution	-	-	543059	-

New result using VQEClient on IBMQ manila: 554568 +/- 1179 (1.90%)

Detailed statistics of SSVQE results

$N_{\max}$	$L_{\max}$	State	Exact energy (MeV^2)	SV sim (MeV^2)	qasm sim (MeV^2)
1	1	$\|00\rangle$	543059	543059 (0%)	543059 ± 0 (0%)
		$\|01\rangle$	593915	593915 (0%)	593915 ± 0 (0%)
		$\|10\rangle$	1686541	1685210 (0.08%)	1686541 ± 70 (0%)
		$\|11\rangle$	1715577	1716743 (0.07%)	1715577 ± 66 (0%)
4	1	$\|0000\rangle$	180012	180802 (0.44%)	189263 ± 6511 (1.08%)
		$\|0001\rangle$	402071	405796 (0.93%)	419139 ± 6324 (1.73%)
		$\|0010\rangle$	493293	499376 (1.23%)	532381 ± 7008 (5.21%)
		$\|0011\rangle$	742530	774189 (4.26%)	745422 ± 6503 (2.88%)

Hamiltonian encoding for $(N_{\max}, L_{\max}) = (4, 1)$

$$
\begin{aligned}
H^{(4,1)}_{\text{compact}} = {} & 1868696\, IIII - 623614\, IIIZ + 518799\, IIXI + 44344\, IIXZ \\
& - 531599\, IIZI + 11950\, IIZZ + 29183\, IYIY - 21316\, IYXY \\
& + 28874\, IYYI + 22502\, IYYX - 1474\, IYYZ + 6301\, IYZY \\
& + 1762\, XXII + 7092\, XXIZ - 310\, XXXI - 4214\, XXXZ \\
& + 653\, XXZI + 3207\, XXZZ + 77283\, XZII - 61720\, XZIX \\
& + 4548\, XZIZ - 38263\, XZXI + 33154\, XZXX - 3510\, XZXZ \\
& + 844\, XZYY + 19387\, XZZI - 15666\, XZZX + 2304\, XZZZ \\
& + 29183\, YIIY - 21316\, YIXY - 28874\, YIYI + 22502\, YIYX \\
& + 1474\, YIYZ + 6301\, YIZY + 1762\, YYII + 7092\, YYIZ \\
& - 310\, YYXI - 4214\, YYXZ + 653\, YYZI + 3207\, YYZZ \\
& - 77283\, ZXII - 61720\, ZXIX - 4548\, ZXIZ + 38263\, ZXXI \\
& + 33154\, ZXXX + 3510\, ZXXZ + 844\, ZXYY - 19387\, ZXZI \\
& - 15666\, ZXZX - 2304\, ZXZZ + 215302\, ZZII - 34396\, ZZIZ \\
& + 70683\, ZZXI + 19390\, ZZXZ - 12936\, ZZZI - 11024\, ZZZZ,
\end{aligned}
$$

Basis encoding for $(N_{\max}, L_{\max}) = (4, 1)$

	n	m	l	s	$\bar{s}$	Compact encoding
1	0	0	0	1/2	-1/2	$\|0000\rangle$
2	0	0	0	-1/2	1/2	$\|0001\rangle$
3	0	0	1	1/2	-1/2	$\|0010\rangle$
4	0	0	1	-1/2	1/2	$\|0011\rangle$
5	0	1	0	-1/2	-1/2	$\|0100\rangle$
6	0	1	1	-1/2	-1/2	$\|0101\rangle$
7	0	-1	0	1/2	1/2	$\|0110\rangle$
8	0	-1	1	1/2	1/2	$\|0111\rangle$
9	1	0	0	1/2	-1/2	$\|1000\rangle$
10	1	0	0	-1/2	1/2	$\|1001\rangle$
11	1	0	1	1/2	-1/2	$\|1010\rangle$
12	1	0	1	-1/2	1/2	$\|1011\rangle$
13	1	1	0	-1/2	-1/2	$\|1100\rangle$
14	1	1	1	-1/2	-1/2	$\|1101\rangle$
15	1	-1	0	1/2	1/2	$\|1110\rangle$
16	1	-1	1	1/2	1/2	$\|1111\rangle$